The EMBO Journal vol.5 no.1 pp.41-49, 1986

Electron microscopy of the low pH structure of influenza virus haemagglutinin

R.W.H.Ruigrok, N.G.Wrigley, L.J.Calder, S.Cusack[1], S.A.Wharton, E.B.Brown and J.J.Skehel

Division of Virology, National Institute for Medical Research, Mill Hill, London NW7 1AA, UK and [1]EMBL Grenoble Outstation, Institut Laue-Langevin, 156X, 38042 Grenoble Cedex, France

Communicated by D.A.Rees

Influenza virus haemagglutinin mediates infection of cells by fusion of viral and endosomal membranes, triggered by low pH which induces a conformational change in the protein. We report studies of this change by electron microscopy, neutron scattering, sedimentation and photon correlation on X-31 (H3N2) haemagglutinin, both intact and bromelain cleaved, in various assemblies. HAs in all preparations showed a thinning at low pH, and a marked elongation which was removed on tryptic digestion, revealing altered features in the remaining stem portion of the molecule. A tentative model of the change is proposed, with reference to the known X-ray structure at neutral pH, in which major changes occur in the stem tertiary structure, while the top portion is only affected in its quaternary structure.

Key words: electron microscopy/influenza virus haemagglutinin/low pH conformational change/membrane fusion/virus entry

Introduction

The haemaggultinin (HA) surface glycoprotein of influenza virus has long been known to have a role in cell attachment of the virus via binding to cell receptors containing sialic acid (Hirst, 1943). It also mediates membrane fusion following an irreversible structural change induced by low pH (see review by White *et al.*, 1983). The fusion of the viral membrane with the membrane of an acidic endosome appears to be an essential step in the infection process.

The complete haemagglutinin molecule (HAo) is synthesized as a single protein chain of some 550 residues which is cleaved during maturation at residue 328 in the case of viruses of the H3 subtype. This results in two polypeptide chains, designated HA_1 and HA_2 (subscripts 1 and 2 refer throughout to these two chains), that remain linked by a disulphide bond. This maturation cleavage, creating the HA_1 C terminus (C_1) and HA_2 N terminus (N_2), is necessary for infectivity of the newly produced virus (Klenk *et al.*, 1975; Lazarowitz and Choppin, 1975) and for the low pH-induced fusion process (Huang *et al.*, 1981; White *et al.*, 1981). The morphological entity on the infectious viral surface is a trimer of (HA_1 + HA_2), it is a rod-shaped spike, which protrudes 13.5 nm from the membrane in which the anchor peptide C_2 is embedded, and has a thickness of ~6 nm, which includes the surface sugars. The protruding portion may be shorn intact from the virion by proteolytic cleavage at residue 175_2 (Brand and Skehel, 1972; Dopheide and Ward, 1981) with bromelain. The product, designated BHA, is soluble and retains its native biological properties. It has been crystallized and its X-ray structure (Figure 1) is known to a resolution of 0.3 nm (Wilson *et al.*, 1981).

Broadly, the trimeric rod consists of an α-helical 'stem' extending some 10 nm from the virus membrane, surmounted by a globular 'top' portion rich in β structure. This top portion contains the antigenic sites and the sialic acid receptor binding site (Wiley *et al.*, 1981).

The HA spikes may also be released intact by detergent disruption of the viral membrane. This complete form of HA (which we designate CHA) still contains the hydrophobic C_2-terminal membrane anchor peptide and aggregates into rosettes immediately upon removal of the detergent.

The altered structure of BHA or CHA following low pH exposure is not known in any detail. It is known for BHA that the hydrophobic N_2-terminal peptide, generated during the maturation cleavage and having strong sequence homology with the fusion peptide of Sendai virus, becomes exposed externally upon lowering the pH, causing the previously soluble BHA to aggregate into rosettes (Skehel *et al.*, 1982). Treatment of these aggregates with thermolysin results in resolubilization of the protein, which requires removal of the N_2-terminal peptide (Daniels *et al.*, 1983b). Furthermore, the HA_1 chain becomes susceptible to trypsin cleavage at residue 27_1 after incubation at low pH, resulting in the release of HA_1 tops as monomers (Skehel *et al.*, 1982). A second trypsin cut occurs with some strains at 224_1. Both this phenomenon and the loss of antigenic sites in the HA_1-HA_1 intra trimer region (Daniels *et al.*, 1983a), suggest an opening of the trimeric structure at the top of the molecule. C.D. measurements have indicated that the secondary structure does not change detectably after low pH (Skehel *et al.*, 1982). This agrees with the fact that most antigenic sites on HA_1, and the sialic acid receptor, remain functional, indicating that the change is not a process of gross denaturation but more a relative movement of domains which maintain their individual structures.

This paper explores the structural correlates of these processes by high resolution low-dose electron microscopy, neutron scattering and hydrodynamic techniques making use of several assemblies and sub-assemblies of BHA and CHA. Since X-ray crystallographic data are unlikely to be forthcoming in the near future, these appear to be the best available means to study the low pH configuration of haemagglutinin.

Results

Exposure of virus to low pH

On native virus particles (Figure 2a) the spikes appeared as rods with a well-defined length of 13.6 ± 0.6 nm (all length measurements of the different forms of HA are summarised in Table I). After treatment at low pH, however, the spikes were no longer visible as separate entities but appeared as a 14.3 ± 2.4 nm thick layer of entangled thin threads (Figure 2b), as reported previously (Ruigrok *et al.*, 1984). Trypsin treatment of these particles (Figure 2c) resulted in a 4 nm shortening of the spikes which could now be seen as separate rods, thinner than a pH 7 spike, sometimes with a small knob at the distal end. Also, neuraminidase molecules could be seen sticking out as

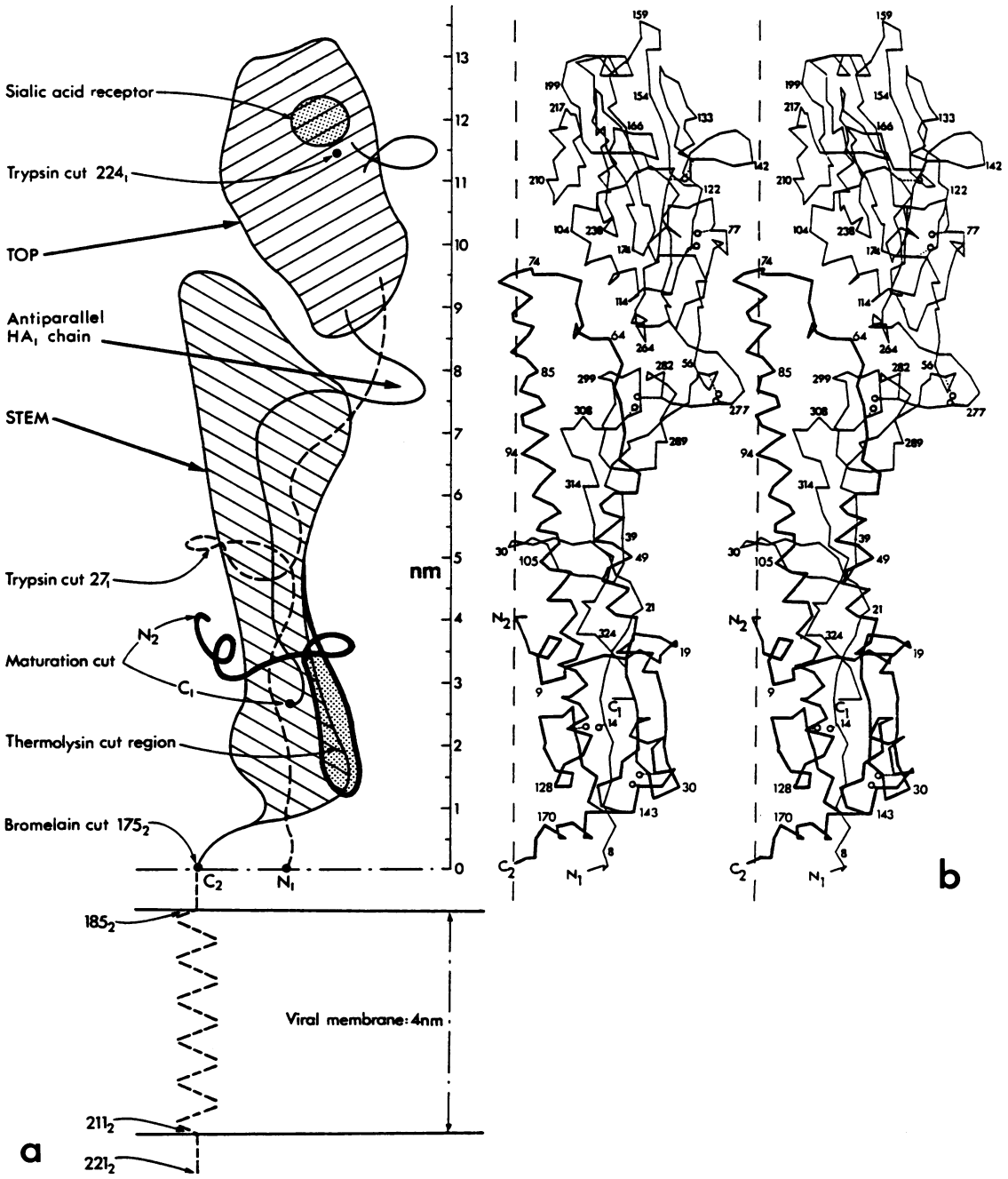

Fig. 1. (**a**) Sketch of the important features and cleavage points of the BHA monomer, namely: (**1**) the C_1 and N_2 termini generated upon maturation cleavage, separated by 2.1 nm, (**2**) the bromelain cut at 175_2, (**3**) the two sites accessible to trypsin after low pH at 27_1 and 224_1, (**4**) the thermolysin cut region of HA_2. Thermolysin does not cut at a unique point but releases the first 23 residues onwards from N_2. The C_2-terminal 46 residues removed by bromelain (the anchor peptide) are drawn arbitrarily in **a**, since they are not included in the BHA crystal. It is noteworthy that the uncharged sequence 185_2-211_2 would exactly span the 4-nm virus membrane as an α-helix, leaving a further 10 residues inside the virion. The apparent thickness of the whole spike is misleading since the surface sugars which contributed to the EM thickness are not shown here. (**b**) α-Carbon backbone of an HA_1 + HA_2 monomer as determined by X-ray crystallography for BHA (Wilson *et al.*, 1981), showing its secondary and tertiary folding in stereo. HA_1 is drawn with a thin line, HA_2 with a thick line. The dashed line on the left of the molecule indicates the 3-fold axis of the trimer.

bulky heads on a thin stalk 14.4 ± 0.9 nm long, apparently unaltered by low pH or trypsin treatments.

Experiments with CHA and virosomes

The dense spike population on virus particles prohibited observation of single molecules. Therefore we studied detergent-released CHA in solution and incorporated sparsely into synthetic liposomes (virosomes). Prepared in the presence of detergent, the CHA pH 7 spike (Figure 4a) has a length of ~20.5 nm. If the whole of the 46-residue C_2 anchor peptide which is cut from HA by bromelain were α-helical, this would represent an extra length of 6.9 nm, making a total spike length of 20.4 nm. After removal of the detergent the rods aggregate into rosettes (Figure 4b) with a diameter of ~37.5 nm, implying a spike overlap at the rosette centre of ~3.5 nm, similar to the thickness of a biological membrane. Inserted in a liposome (Figure 3a), the

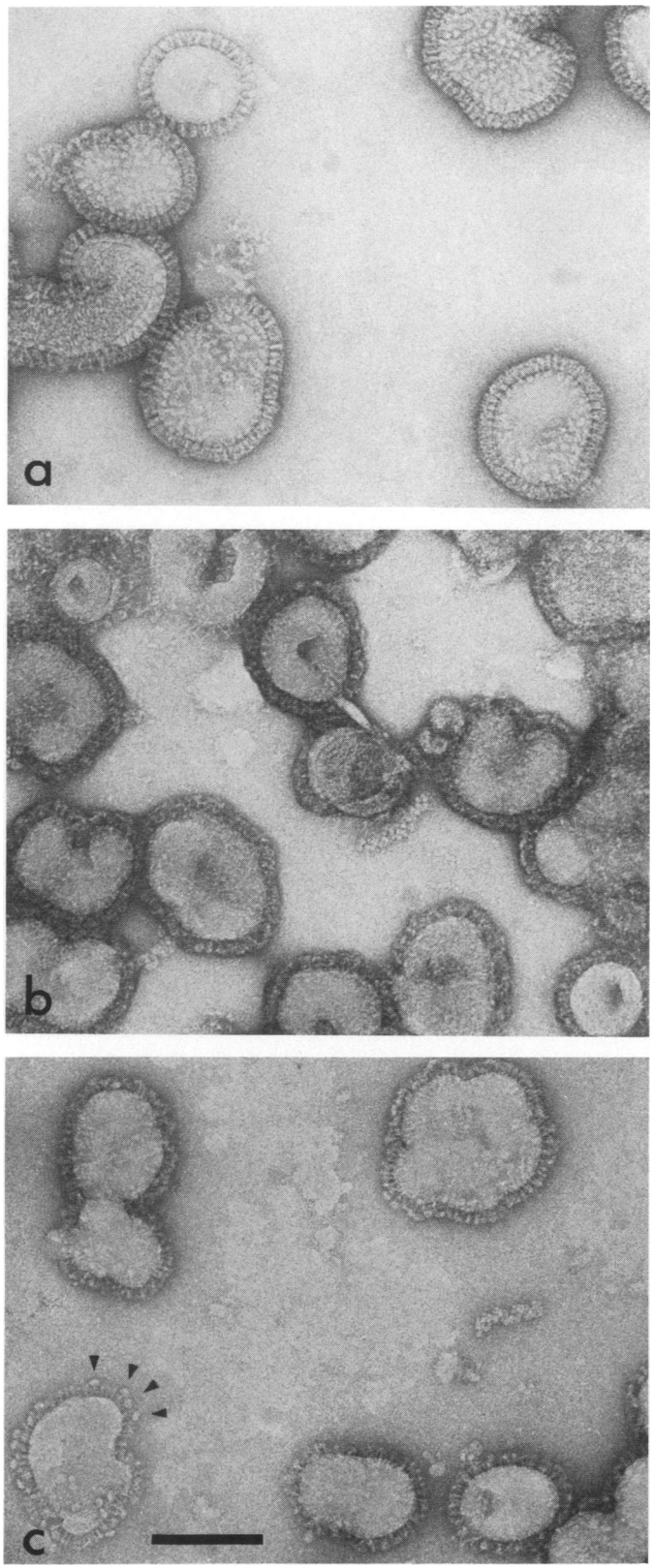

Fig. 2. Particles of strain X31 influenza virus (**a**) at pH 7 showing ordered surface spikes, (**b**) after exposure to low pH showing a fuzzy disordered surface fringe, and (**c**) after low pH and trypsin digestion, showing thinned surface spikes of well-defined length, except for the unaltered neuraminidase molecules (arrowed). Bar = 100 nm.

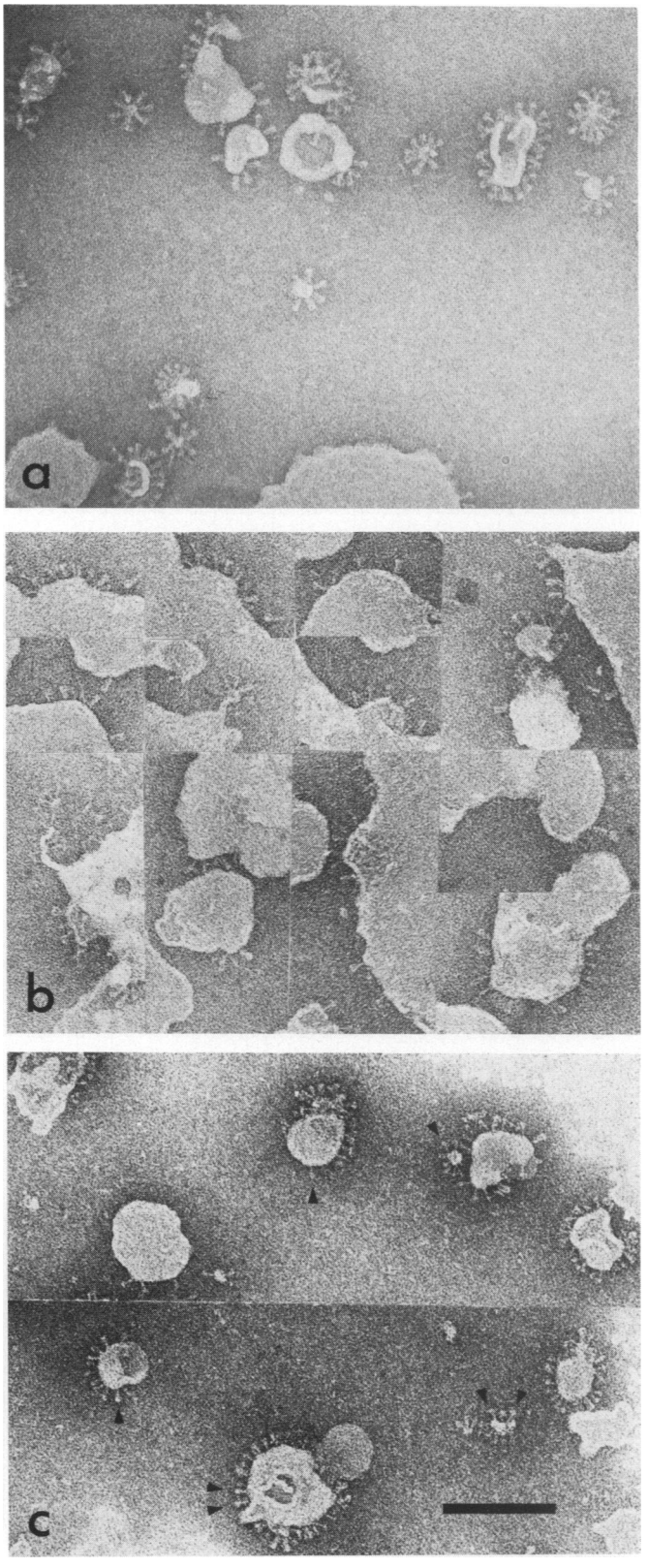

Fig. 3. Synthetic virosomes with HA spikes, (**a**) at neutral pH, (**b**) after low pH showing mostly thinned extended and/or branched spikes, and (**c**) after low pH and trypsin showing some terminal knobs (arrowed). Bar = 100 nm.

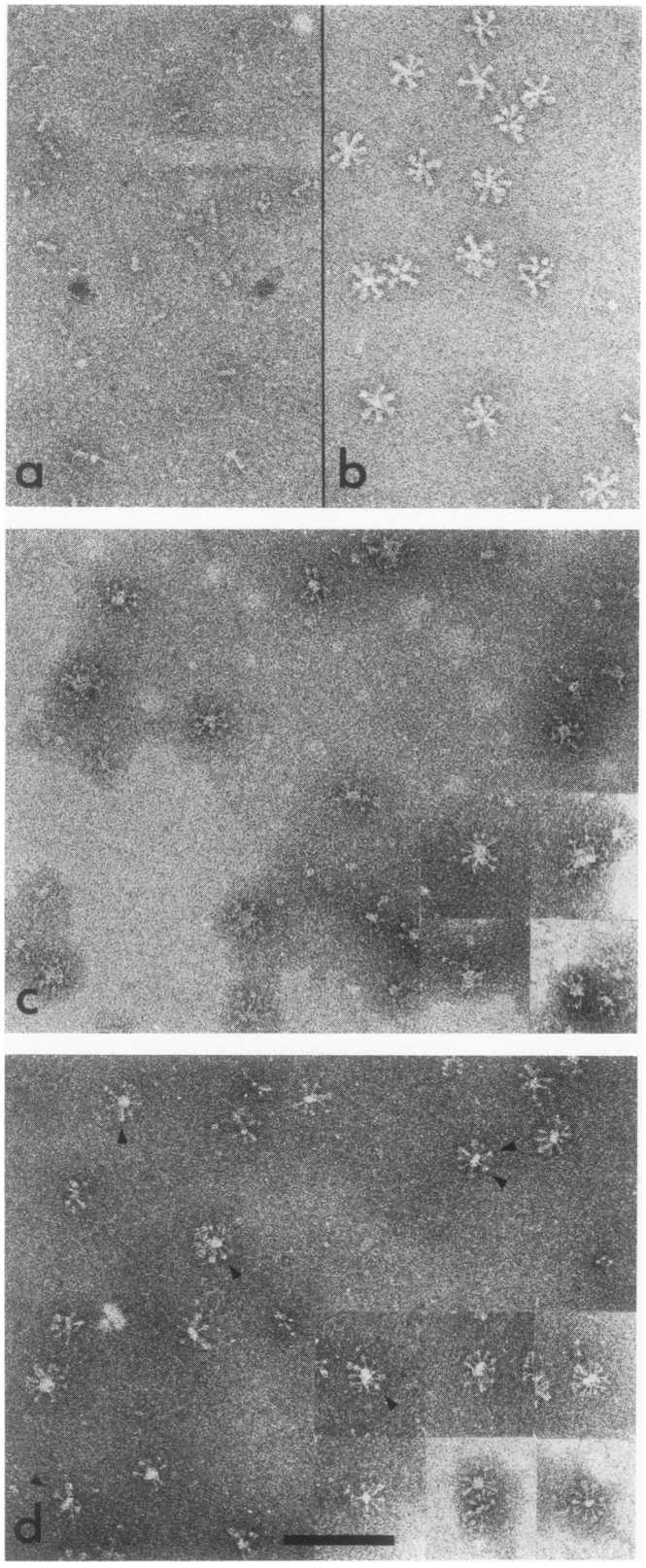

Fig. 4. (**a**) Single CHA molecules in the presence of 0.5% Lubrol and (**b**) the same as rosettes after removal of the detergent. (**c**) The rosettes after low pH exposure, showing thinned and lengthened spikes. (**d**) The same after trypsin; the thinned spikes are shorter again and the terminal knobs (arrowed) are more evident than in (**c**). Note enlarged rosette centres in (**c**) and (**d**) compared with BHA rosettes. Bar = 100 nm.

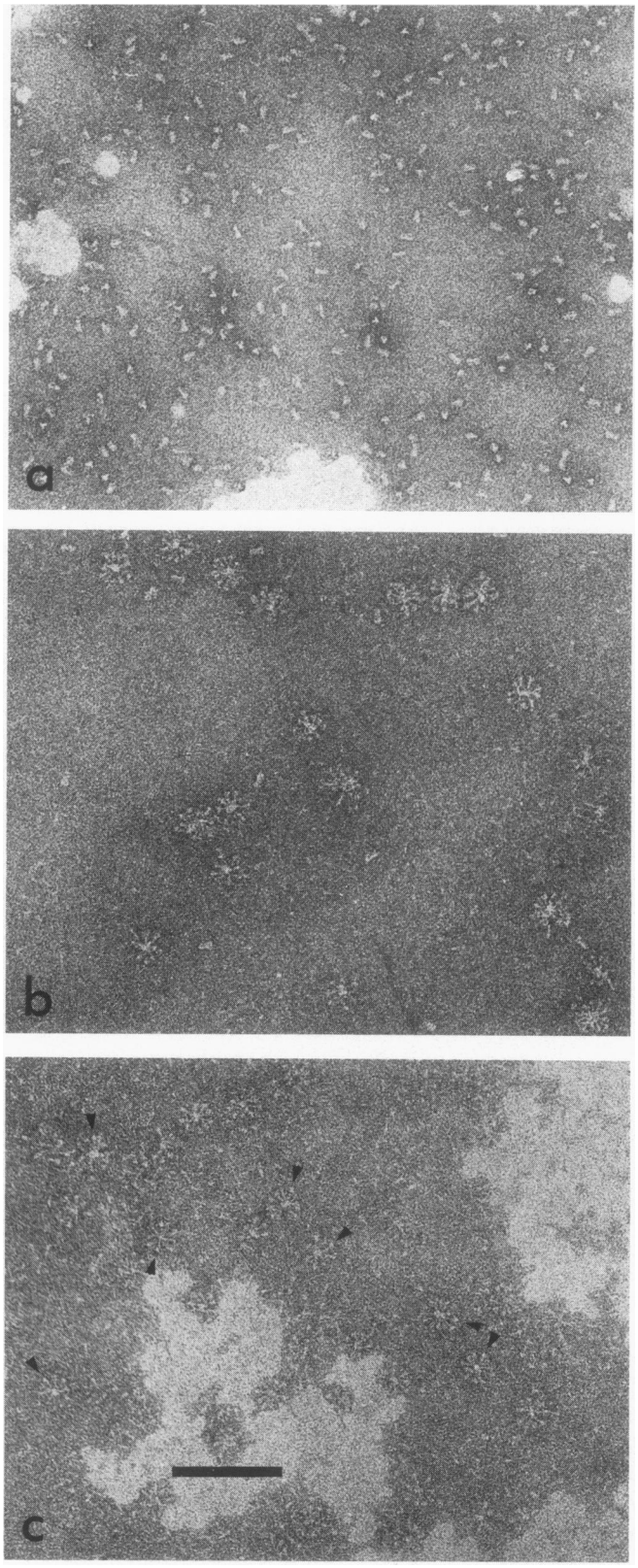

Fig. 5. Molecules of BHA (**a**) at neutral pH showing side views and some triangular end views, (**b**) aggregated into rosettes after low pH showing thinned extended spikes, and (**c**) after low pH and trypsin; terminal knobs (arrowed) are more evident than in (**b**). Bar = 100 nm.

Table I. Summary of the length measurements on the different types of X-31 HA assemblies before and after exposure to low pH and trypsin

Type of HA and assembly	Length measurements in nm			
	pH 7	low pH	low pH + trypsin	branch point after low pH
HA on virus	**13.6**[a]	**14.3**[b]	**10.4**[a]	–
	13.6±0.6 (54)	14.3±2.4 (125)	10.4±0.8 (42)	
CHA as singles[c]	**20.5**	–	–	–
	20.5±1.5 (125)			
in rosettes	**18.7**[d]	**21.1**[d]	**17.6**[d]	–
	18.1±0.9 (40)	21.1±1.9 (94)	17.6±1.0 (70)	
	18.9±0.9 (96)			
on virosomes	**13.8**[a]	**15.5**[a,e,f]	**10.8**[a]	**10.0**[g]
	13.7±0.6 (110)	17.6±2.4 (87)	10.8±1.0 (177)	9.8±0.9 (43)
	13.9±0.7 (63)	15.2±2.9 (116)		10.0±0.7 (107)
		13.9±2.2 (131)		10.0±1.2 (93)
BHA as singles	**13.7**	–	–	–
	13.7±0.4 (204)			
in rosettes	–	**17.2**[d,e]	**15.1**[d]	**10.0**[h]
		17.1±0.9 (91)	15.0±0.8 (79)	9.5±1.0 (74)
		17.2±1.9 (53)	15.1±1.1 (92)	10.5±1.3 (136)
		17.4±1.0 (74)	15.2±0.8 (38)	

Averages of length measurements of HA molecules are shown in bold type, together with individual measurements and standard deviations plus the number of units measured in brackets.
[a]Measured from membrane to top of discrete molecules.
[b]Measured from virus membrane to top of spike layer.
[c]Prepared in the presence of 0.5% Lubrol.
[d]Radius of rosette, derived from diameter measurements in two directions.
[e]Excluding the very long extensions.
[f]This result was extremely variable.
[g]Measured from membrane to branch point or beginning of knob.
[h]Measured from centre of rosette to branch point or beginning of knob.

CHA molecule showed as a spike, 13.8 nm long, as on native virus. Low pH treatment of CHA rosettes and virosomes (Figure 4c and 3b, respectively) resulted in a thinning and lengthening of the spikes by some 2 nm in both cases. Most notably the variability in spike length increased, especially on the virosomes (see standard deviations in Table I). Also, the centres of low pH CHA rosettes became enlarged. In both cases many of the spikes showed knobs and/or one or more extensions of variable length at their distal ends. On the low pH virosomes both the knobs and the branching started ~10 nm from the membrane. After trypsin treatment both kinds of assemblies (Figure 4d and 3c) showed a decrease in spike length of some 4 nm. The resulting, shortened spikes looked very much like the spikes on viruses after low pH and trypsin, that is, thin and often with a small distal knob.

In summary, the spike lengths on virus, CHA rosettes and virosomes increased by 1–2 nm at low pH, and decreased by some 4 nm upon trypsin digestion. This decrease would be consistent with the loss of tops, which at pH 7 contribute 4 nm to the total spike length (Figure 1). However, the trypsin cut was made on the extended low pH form; if the low pH extension had been due only to unfolding/elongation of the tops then the loss would have been 5–6 nm. Since the decrease was only 4 nm, some element other than tops must have lengthened at low pH.

Experiments with BHA

BHA is soluble at pH 7, as shown in Figure 5a. The truncated spike length was 13.7 nm which is in excellent agreement with the value of 13.5 nm determined from the X-ray structure (Figure 1), with the protruding spike lengths measured on virus and virosomes, and with a recent measurement of 13.7 nm using cryomicroscopy (Booy *et al.*, 1985). After low pH, BHA associates into rosettes composed of thin spikes radiating from the centre (Figure 5b); extensive counts showed a total of 8 ± 1 spikes on average per rosette (range 6–12) assumed to be flattened in drying down for microscopy. However, some rosettes seemed too crowded for spike counts and these may have had >12 spikes. The formation of BHA rosettes is a consequence of the extrusion of the N_2 region (Skehel *et al.*, 1982; Daniels *et al.*, 1983a), but the detailed configuration of this aggregation and any information of spike overlap at the rosette centre are unknown. Assuming zero overlap, the spike length increased by 3.7 nm at low compared with neutral pH, considerably more than the average increases observed for CHA and HA in virus at low pH.

Apart from electron microscopy, we also performed neutron scattering and combined sedimentation and photon correlation experiments. The sedimentation experiments showed that native BHA and low pH BHA in 0.2% Lubrol behaved as a single molecular species of 8.4S and that BHA rosettes sedimented as a complex of 28S (Table II). From a combination of these measurements with the diffusion coefficient measured by photon correlation (Table II) it can be calculated (see Materials and methods) that a BHA rosette contains ~9 BHA trimers (cf. 8 ± 1 from EM, above). It is noteworthy that the hydrodynamic radius of the BHA rosettes, 17 nm as derived from the diffusion coefficient, is very similar to the 17.2 nm radius determined by EM.

Small-angle neutron scattering experiments were performed on pH 7 BHA, low pH BHA rosettes and low pH BHA in the presence of 0.2% Lubrol. The mol. wt. of pH 7 BHA was found to be (2.27 ± 0.22) × 10^5 daltons and the radii of gyration in

Table II. Summary of the results of sedimentation analysis and photon correlation spectroscopy

Sample	Sedimentation coefficient	Hydrodynamic radius[a]	Diffusion coefficient[b]
Native BHA	8.4 ± 0.1S	6.0 ± 0.5 nm	3.49 ± 0.3
BHA rosettes	28.0 ± 1.0S	17 ± 0.8 nm	1.26 ± 0.06
Low pH BHA in 0.2% Lubrol	8.3 ± 0.3S	6.1 ± 1.6 nm	3.47 ± 0.7

All results are the averages of three separate experiments.
[a]Derived from the diffusion coefficient.
[b]$D_{20,w}$, in $cm^2/s \times 10^{-7}$.

H_2O and D_2O were, respectively, 4.37 ± 0.11 nm and 3.97 ± 0.13 nm. These values are slightly higher than expected from the known mol. wt. (2.09×10^5) and radius of gyration (3.72 nm in H_2O) calculated from the crystal structure (Wilson *et al.*, 1981) indicating some aggregation in solution. This was also observed in the photon correlation experiments.

The mol. wt. of BHA rosettes was measured to be (15.4 ± 0.24) $\times 10^5$ daltons and the radii of gyration in H_2O and D_2O were, respectively, 12.4 ± 0.2 nm and 12.9 ± 0.1 nm. The mol. wt. corresponds to an aggregate of ~7 BHA molecules.

If we approximate the form of pH 7 BHA as a cylinder of length 13.5 nm (as given by the crystal structure), then a radius of 3 nm gives the observed radius of gyration (*R*g) in H_2O (~4.4 nm). Supposing that low pH BHA is a rosette of 7–9 BHA molecules projecting out radially, then a spherical rosette of 13.5 nm radius would have an *R*g of 10.5 nm, well below the *R*g of 12.4 nm measured for low pH BHA.

Alternatively, let us suppose that, at low pH, BHA molecules can become longer (to 16.5 nm) and more slender (to 2.5 nm radius). Then a single molecule would have an *R*g of 5.1 nm, which is close to the value of 5.17 ± 0.21 nm measured for the low pH BHA-Lubrol complex in 10% D_2O at which contrast the scattering is essentially from the protein alone. The spherical rosettes would have an *R*g of 12.8 nm which is close to the *R*g actually measured. Further, the spherical rosette would have a hydrodynamic radius of ~16.5 nm in accord with the photon correlation and EM measurements. Also, an *R*g of 5.1 nm for soluble low pH BHA in Lubrol indicates that this molecule cannot be much larger than 16.5–17 nm since

$$Rg = \frac{l^2}{12} + \frac{r^2}{2}$$

(l and r are the length and radius of a cylinder respectively) which suggests that the molecules in the BHA rosettes do not overlap significantly.

Low pH BHA before and after trypsin treatment

Figure 6 shows selected BHA rosettes with sketches of our interpretations. As mentioned above, an average number of 8 ± 1 thin spikes could be seen joined in each rosette. The results of the sedimentation, photon correlation and neutron experiments suggest that these spikes must be interpreted as trimers, despite their slenderness. Most of the spikes were found to branch or carry knobs at a distance of 10 nm from the rosette centre, equal to the branch point of CHA in virosomes. Up to three branches could be seen and occasionally very long extensions (average 26 ± 3 nm). Often the branched molecules contained a knob starting at 10 nm but it was not clear whether this knob was of the same size as on the molecules with knobs only, namely 5 nm radially, on top of the 10 nm stem, giving a rosette radius of

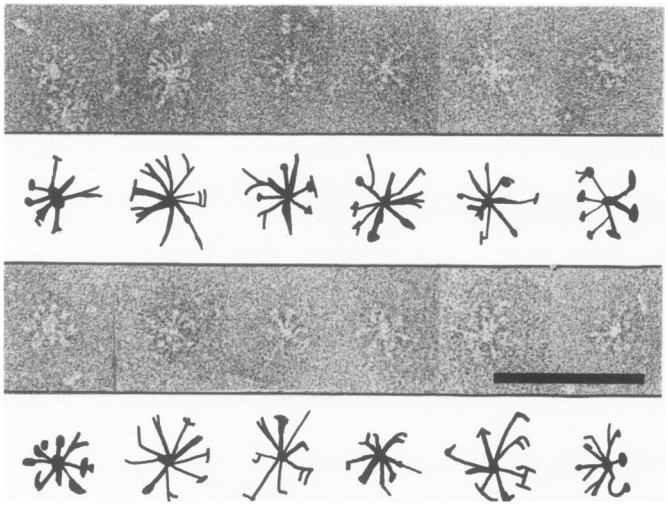

Fig. 6. Selected rosettes of low-pH BHA (as in Figure 5b), showing thinned and elongated spikes, some with knobs and branches. The sketches below each frame are only intended to illustrate the kind of detail discussed. Bar = 100 nm.

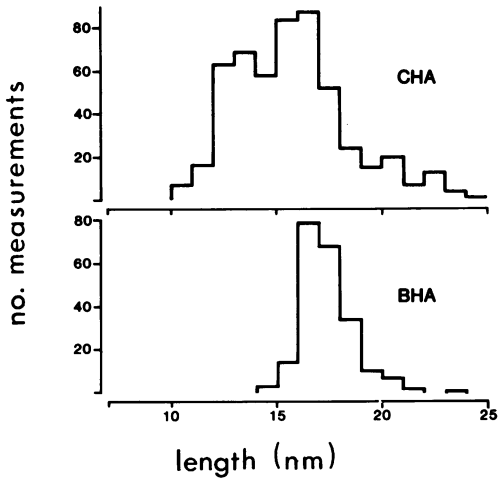

Fig. 7. Length distribution of CHA spikes on virosomes after low pH, compared with BHA in low pH rosettes. The latter assumes zero spike overlap at the rosette centre.

15 nm. The low pH CHA on virosomes showed a similar range of modified structures although the range in the length measurements of these molecules was much larger than the range for low pH BHA (Figure 7). It should be noted that the diameter measurements on BHA rosettes did not include the very long extensions.

Trypsin treatment of BHA rosettes (Figure 5c) again resulted in a shortening of the spikes, but only by 2.2 nm compared with ~4 nm in CHA. That is, there was a net gain instead of a net loss after the low pH and trypsin treatments. This shows a clear difference between BHA and CHA. As with the CHA spikes, the trypsin digestion removed the long extensions and branches present on the BHA rosettes leaving smaller rosettes still composed of 8 ± 1 thin spikes. About half the spikes showed a small distal knob which extended to 15 nm but which started only at 11.3 nm. However, spikes with or without knobs were of the same length, indicating that the apparent presence or absence of the small knob may have been influenced by staining variations.

Discussion

General

In this paper we describe studies on several assemblies of HA in the low pH conformation, using a number of different techniques. The results of the EM experiments on BHA and the neutron scattering plus sedimentation/photon correlation results are in good agreement. The similarities of the measured BHA rosette radii and the number of spikes found per rosette provide evidence that neither the EM nor neutron scattering data were subject to significant preparation artefacts or interpretation failures. Furthermore, the agreement on numbers of spikes per rosette indicates that the thin spikes and their branched structure observed with EM must be interpreted as trimers and not as the monomers their thinness might have suggested. The thinning of the spikes seen in negative stain might be due to differential penetration of the stain in the native and low pH forms of the protein but was also independently deduced from the neutron scattering data (Results). The results showed that both the pH 7 BHA and the BHA rosettes formed at pH 5 were very homogeneous, indicating that BHA rosette formation may be subject to either symmetry or steric limitations.

Trypsin treatment

We assume that the orientation of the spike molecules in the BHA rosettes is unique, that is, the same end of the molecule is always situated in the centre of the rosette and the aggregation site is at one extreme end of the molecule. The position of the branch point in both BHA and CHA molecules was 10.0 nm from the rosette centre or the virosome membrane respectively. From this point onwards branching and/or unwinding of the molecule took place. This suggests that the spikes in the BHA rosettes were oriented with their former membrane ends in the rosette centre. We have carefully explored the alternative possibility of top-to-top aggregation (see below).

Incubation of low pH X-31 HA with trypsin results in cleavage at Lys 27_1 and secondarily at Arg 224_1 (Skehel *et al.*, 1982). This removes the major part of HA_1 (residues 28_1-328_1 = 'tops') from the rest of the spike. With EM it was observed that the spikes lost their branches and long threads, which we therefore interpreted as tops, unfolded and disassociated from each other, and that the remainder was a thin rod with or without a small knob. This is consistent with the 4 nm length reduction of CHA after trypsin. It seems clear that the trimeric contacts in tops are broken after low pH and that additional unfolding in some 10% of the spikes may occur producing the long threads. It is not clear whether this additional unfolding is reversible or not, or whether it results from staining and air-drying on the grid.

After trypsin treatment, the BHA molecule in the rosette was 15 nm long while the CHA molecule on the virosome and HA on virus was only some 10.5 nm. This is a major difference between the two kinds of molecules. Analysis of the length measurements of the pre-trypsin low pH forms also reflected this difference; Figure 7 shows histograms of the length distribution of low pH BHA and CHA molecules. The BHA lengths range from ~15 to 21 nm and CHA from 10 to 23 nm. With low pH CHA this resulted in a lower average and a larger standard deviation than for BHA. This suggests that in low pH BHA spikes, where the 5 nm knob extending to 15 nm radius was not obvious, the knob might nevertheless be present but interpreted as one of the branches. After trypsin treatment of BHA rosettes the knob was smaller, extending from 11.3 to the same 15 nm radius. This suggests that in pre-trypsin low pH BHA the 5 nm knob (from 10 to 15 nm) consists of an HA_2 segment (11.3 – 15 nm) partly overlapping with HA_1 tops (10.0 – 11.3 nm or more, but not longer than 15 nm).

Proposed model of the low pH conformation of BHA

The terminal knobs in BHA rosettes were present after trypsin treatment, so they must be part of HA_2, since only N_1 to 27_1 of HA_1 remains, disulphide-linked at 14_1. This indicates that at low pH major structural changes take place in BHA_2. A possible model for the conformational change in BHA would be the following: the N_2 terminus folds out of the hydrophobic pocket near the trimer axis and moves towards the bottom of the molecule where it interacts with other N_2 termini, forming base-to-base rosettes. The region of β structure from 22_2 to 38_2 unwinds [becoming susceptible to thermolysin (Daniels *et al.*, 1983a)] and moves upwards together with the small HA_2 stem helix and also the HA_1 part of the stem. Movement of the latter is possible by unwinding the 22_1-37_1 loop (Figure 1a) which becomes susceptible to trypsin cleavage after pH 5 incubation; the C_1 terminus is relatively free to move. The N_1 terminus remains in place as it is linked via a disulphide bridge to the β region at the foot of the long α-helix. All this movement can explain our three major observations: (i) the stem clearly becomes much thinner with the migration of so much material upwards; (ii) the small stem helix plus associated chain of HA_2 are now available at the top of the remaining stem to become the observed knob extending to a radius of 15 nm; (iii) the branch point for opening of the trimeric tops is now also at 10 nm radius as observed. Destabilization of the tertiary and quaternary contact between tops-tops and tops-HA_2 may result in destruction of the intermonomer antigenic sites and will allow the tops to be released from the remainder of the molecule when the trypsin cut is made.

Amino acid substitution in a number of regions of the molecule appear to influence its stability (Daniels *et al.*, 1985). These include: (i) the N_2 terminus (3_2, 6_2, 9_2, 17_1, 112_1 and 114_1); (ii) the trypsin-cut loop (105_2); (iii) the HA_2 small helix (47_2, 51_2, 54_2 and 57_2) and (iv) the interface between HA_1 and the top of the HA_2 stem (91_1 and 300_1). All these regions are implicated in the proposed conformational change.

Comparison of BHA and CHA

The conformational changes in BHA and CHA at low pH appear to be the same. The branch points in both were at 10 nm; both showed up to three branches and very long extensions, and both had the same highly restricted susceptibility to tryptic digestion (Daniels *et al.*, 1983b). The real differences between BHA and CHA appeared to be in HA_2, and were especially obvious after trypsin: BHA_2 extended to 15 nm and CHA_2 to only 10.5 nm, though this was still longer than the 9.5 nm at pH 7 (Figure 1). Also, the distal knobs appeared somewhat smaller on CHA_2, though stems were thinned in both, suggesting similar but not identical upwards movement of HA_2 material. All this indicates much similarity between BHA and CHA in the low pH changes and we therefore suggest that the underlying idea of HA_2 movement relative to the long helix backbone applies to both systems, differing only in extent but triggered by the same low pH-induced mechanism.

The small but clear differences between BHA_2 and CHA_2 could result from a relative restriction of the upwards movement in the latter due to one or both of the two differences at the membrane ends of the molecules. (i) In BHA there is no membrane or anchor peptide, and the bromelain cleavage could have caused destabilization in this area, allowing greater movement of non-backbone parts of HA_2. (ii) In CHA in virosomes the low pH extruded N_2 terminus could become embedded in its own mem-

brane (see below), perhaps involving a greater chain length than in BHA N_2-N_2 rosette aggregation, and so restrict upwards movement. Put differently, if 4–5 nm of the CHA N_2 chain were embedded in its own viral membrane, then that much less length would be free to move upwards to form the distal knob which we found in BHA extending to 15 nm.

The position of the N_2 terminus in the low pH conformation

BHA aggregates into rosettes at low pH, and these aggregates are resolubilized upon thermolytic removal of the N_2-terminal 23 residues (Daniels *et al.*, 1983a). The implication of these results is that rosettes are formed by N_2-N_2 association. Where are the N_2-termini located at low pH? We discuss three possibilities: (i) side-to-side aggregation, (ii) top-to-top aggregation and (iii) base-to-base aggregation.

(i) Interactions of the exposed N_2 termini located 3.5 nm from the membrane end of BHA would result in side-to-side association possibly leading to linear or branched chain formation. Such chains were never seen; we only observed well-defined rosettes. Formation of rosettes is easiest to imagine as association of spikes by one extreme end (see points ii and iii). However, it is also possible that side-to-side aggregation, in which specific curvature of these chains is involved, could lead to the formation of small spherical aggregates like our rosettes. This specific curvature could result in some way from the trimeric (and therefore trivalent) nature of BHA.

(ii) From considerations of possible mechanisms of membrane fusion and the role of the HA in the process, it is plausible to suggest that, at the pH of endosomes, N_2 termini migrate towards the distal (non-membrane) ends of the HA to interact with the endosomal membrane. HA might thus provide a direct link between target membrane and viral membrane in which the C_2-terminal hydrophobic anchor is still embedded. The experiments reported here do not include examination of these possibilities since no target membrane was included. However, in CHA rosettes the orientation of the spikes is known with certainty. We observed that these do not aggregate at low pH, suggesting that *in vitro*, N_2 termini do not migrate in a distal direction. Instead CHA rosette centres become enlarged, suggesting a central deposit of more material or more stain-excluding hydrophobicity.

(iii) The third possibility is that the N_2 terminus is directed towards the membrane end of the molecule at low pH. This would result in base-to-base aggregation in BHA rosettes, additional base-to-base interactions in CHA rosettes and possibly N_2 terminus/virus-membrane interactions in isolated virus particles incubated at low pH.

Discrimination between the first and third of these possibilities is not possible at the present level of resolution but the uniform diameter and constant number of molecules in BHA rosettes suggest that the spikes are bound to each other by one end.

The main purpose of structural studies of haemagglutinin in the low pH conformation is to understand how the altered molecular structure mediates membrane fusion. Our results show that the HA becomes extended and thinner after exposure to low pH. They also suggest that, in virus particles, the N_2 termini, which are thought to be involved in fusion, interact with the virus membrane. It is certainly possible that membrane fusion may require similar haemagglutinin/virus-membrane interactions to occur but experiments involving direct observations of virus/target-membrane association will be required to assess their significance in the fusion process.

Materials and methods

Virus and HA preparations

X-31 (H3N2) influenza virus was grown in embryonated hens eggs and purified as described (Skehel *et al.*, 1982). BHA was released from virus by digestion with bromelain and purified (Skehel *et al.*, 1982). CHA was extracted from virus by adding 1 volume of virus (~10 mg/ml viral protein in 0.15 M NaCl, 0.01% sodium azide, 10 mM Tris-HCl pH 8) to 10 volumes of 15 mM Tris-HCl pH 8, 0.5% (w/v) Brij 36T and incubating for 30 min at 4°C. After centrifugation at 100 000 *g* for 60 min, the supernatant, which contained only virus glycoproteins, was passed down a protein A-Sepharose 4B column to which anti-neuraminidase monoclonal antibodies had been bound, in order to remove the neuraminidase. Brij 36T was exchanged for octyl glucoside by centrifugation through a 10–30% sucrose gradient containing 1% (w/v) octyl glucoside for 18 h at 100 000 *g* at 20°C (Wharton *et al.*, 1986).

Virosomes were prepared by dissolving 5 mg lipid extracted from chick embryo fibroblasts (Folch *et al.*, 1957) with 0.16 mg CHA in 5 ml ST buffer (0.15 M NaCl, 10 mM Tris-HCl pH 7.8), supplemented with 2% (w/v) octyl glucoside (Sigma). This mixture was dialysed against numerous changes of small volumes of ST buffer, the final changes were large volumes containing 25 g Amberlite XAD-2 beads to adsorb any residual detergent. All dialyses were carried out at 4°C. CHA rosettes were prepared by rapid dilution of 100 μg CHA in 300 μl ST buffer plus 1% (w/v) octyl glucoside with 10 ml ST buffer lacking the detergent, giving rosettes containing fewer CHA molecules than when this dilution step was omitted. This was then dialysed against two changes of 5 litres ST buffer containing Amberlite beads.

Low pH and trypsin treatments

Virus and BHA preparations in PBS (0.15 M NaCl, 10 mM sodium phosphate, pH 7.3) and CHA preparations in ST buffer were adjusted to pH 5, well below the pH threshold for the conformational change, by addition of 0.2 M sodium citrate, incubated for 10 min and readjusted to pH 7.3 with a 1 M Tris solution. These preparations were either examined directly by EM or incubated with trypsin (Sigma) for 20 min at room temperature in a 1:40 ratio of trypsin to HA by weight. The tryptic products were analysed on 16.5% polyacrylamide gels as described (Skehel *et al.*, 1982). The trypsin digestion was fully effective and it should be noted that, in all cases tested, the released globular HA_1 'tops' were found free in solution by ultracentrifugation.

Electron microscopy

Preparations were made by adsorbing the sample to carbon film and negative staining with 1% sodium silico tungstate (pH 7). Samples were critically diluted by repeated trial and error to optimize spreading. Low pH forms were normally treated with the citrate buffer in free solution before adsorption to the carbon. However, some virosome preparations were treated after adsorption to the carbon film by floating on the low pH buffer. The observed molecular shapes were similar to those of the pre-treated virosomes. In some instances, native BHA molecules were mixed with the other samples to serve as an internal standard and to promote stain spreading.

Micrographs were taken under minimum dose and accurate defocus conditions to preserve real detail to ~1.5 nm (Wrigley *et al.*, 1983). The microscope (JEOL 100C) was operated at 100 kV and its magnification calibrated regularly with catalase crystals. Molecular length measurements were made from × 150 000 prints. Additional magnification of × 10 with a graticule eyepiece ensured that the error in measuring was smaller than the variability of the molecules.

Sedimentation and photon correlation experiments

The experiments were performed in PBS at a protein concentration of 2 mg/ml for sedimentation analysis and 0.02 mg/ml for photon correlation work. Sedimentation analysis was carried out in an MSE Centriscan 75 analytical centrifuge at 20°C running at 25 000 r.p.m. for analysis of BHA low pH rosettes and at 40 000 r.p.m. for native BHA and low pH BHA plus 0.2% Lubrol PX (Sigma). Sedimentation was monitored using Schlieren optics at 8-min intervals. The experimentally obtained S-values were not corrected to $S^0_{20,w}$ because $\bar{\nu}$ of the specimens was not measured. The hydrodynamic radius and the diffusion coefficient (D) of BHA in its different states were determined by photon correlation using the apparatus described by Zulauf and Eicke (1979). Comparison of the low pH rosette mass with the pH 7 BHA mass (subscripts 5 and 7, respectively) was made using: $M = sRT/D(1-\bar{\nu}\varrho)$ (Cantor and Schimmel, 1980); assuming $\bar{\nu}_5 = \bar{\nu}_7$ this gives $M_5/M_7 = s_5D_7/s_7D_5$.

Neutron scattering

Small-angle neutron scattering experiments were performed on instruments D17 and D11 at the Institute Laue-Langevin [in 'Neutron research facilities at the ILL high flux reactor', ILL, Grenoble, France (1983)] on samples of pH 7 BHA,

BHA rosettes, and the low pH form of BHA solubilised in 0.2% Lubrol PX. Protein concentrations were in the range 3–5 mg/ml and all samples were in PBS buffer (pH 7) at various D_2O/H_2O ratios. Additional measurements were made on 1% solutions of Lubrol. Scattering curves were corrected and analysed by standard procedures to derive mol. wts., radii of gyration and match-points (Jacrot, 1976; Jacrot and Zaccai, 1981).

Acknowledgements

Part of this work was supported by the Netherlands Foundation for Chemical Research (S.O.N.) (R.W.H.R. while working at the Biochemical Laboratory, State University, Leiden, The Netherlands).

References

Booy,F.P., Ruigrok,R.W.H. and van Bruggen,E.F.J. (1985) *J. Mol. Biol.*, **184**, 667-676.

Brand,C.M. and Skehel,J.J. (1972) *Naure New Biol.*, **238**, 145-147.

Cantor,C.R. and Schimmel,P.R. (1980), *Biophysical Chemistry*, published by W.H.Freeman and Company, San Francisco, p.607.

Daniels,R.S., Douglas,A.R., Skehel,J.J., Waterfield,M.D., Wilson,I.A. and Wiley,D.C. (1983a) in Laver,W.G. (ed.), *The Origin of Pandemic Influenza Viruses*, Elsevier, NY, pp. 1-7.

Daniels,R.S., Douglas,A.R., Skehel,J.J. and Wiley,D.C. (1983b) *J. Gen. Virol.*, **64**, 1657-1662.

Daniels,R.S., Downie,J.C., Hay,A.J., Knossow,M., Skehel,J.J., Wang,M.L. and Wiley,D.C. (1985) *Cell*, **40**, 431-439.

Dopheide,T.A. and Ward,C.W. (1981) *J. Gen. Virol.*, **52**, 367-370.

Folch,J., Lees,M. and Sloane-Stanley,G.N. (1957) *J. Biol. Chem.*, **226**, 497-507.

Hirst,G.K. (1943) *J. Exp. Med.*, **78**, 99-109.

Huang,R.T., Rott,R. and Klenk,H.-D. (1981) *Virology*, **110**, 243-247.

Jacrot,B. (1976) *Rep. Progr. Phys.*, **39**, 911-953.

Jacrot,B. and Zaccai,G. (1981) *Biopolymers*, **20**, 2413-2426.

Klenk,H.-D., Rott,R., Orlich,M. and Blodorn,J. (1975) *Virology*, **68**, 426-439.

Lazarowitz,S.G. and Choppin,P.W. (1975) *Virology*, **68**, 440-454.

Ruigrok,R.W.H., Cremers,A.F.M., Beyer,W.E.P. and de Ronde-Verloop,F.M. (1984) *Arch. Virol.*, **82**, 181-194.

Skehel,J.J., Bayley,P.M., Brown,E.B., Martin,S.R., Waterfield,M.D., White, J.M., Wilson,I.A. and Wiley,D.C. (1982) *Proc. Natl. Acad. Sci. USA*, **7**, 968-972.

Wharton,S.A., Skehel,J.J. and Wiley,D.C. (1986) *Virology*, in press.

White,J., Matlin,K. and Helenius,A. (1981) *J. Cell. Biol.*, **89**, 674-679.

White,J., Kielian,M. and Helenius,A. (1983) *Q. Rev. Biophys.*, **16**, 151-195.

Wiley,D.C., Wilson,I.A. and Skehel,J.J. (1981) *Nature*, **289**, 373-378.

Wilson,I.A., Skehel,J.J. and Wiley,D.C. (1981) *Nature*, **289**, 366-373.

Wrigley,N.G., Brown,E.B. and Chillingworth,R.K. (1983) *J. Microsc.*, **130**, 225-232.

Zulauf,M. and Eicke,H.-F. (1979) *J. Phys. Chem.*, **83**, 480-486.

Received on 7 October 1985; revised on 14 November 1985